PHYSICAL REVIEW D **83,** 106006 (2011)

Searching for string resonances in e^+e^- and $\gamma\gamma$ collisions

Luis A. Anchordoqui,[1] Wan-Zhe Feng,[2] Haim Goldberg,[2] Xing Huang,[1] and Tomasz R. Taylor[2]
[1]*Department of Physics, University of Wisconsin-Milwaukee, Milwaukee, Wisconsin 53201, USA*
[2]*Department of Physics, Northeastern University, Boston, Massachusetts 02115, USA*
(Received 16 December 2010; published 16 May 2011)

If the fundamental mass scale of superstring theory is as low as a few TeVs, the massive modes of vibrating strings, Regge excitations, will be copiously produced at the Large Hadron Collider (LHC). We discuss the complementary signals of low-mass superstrings at the proposed electron-positron facility (CLIC), in e^+e^- and $\gamma\gamma$ collisions. We examine all relevant four-particle amplitudes evaluated at the center-of-mass energies near the mass of lightest Regge excitations and extract the corresponding pole terms. The Regge poles of *all* four-point amplitudes, in particular, the spin content of the resonances, are completely model-independent, universal properties of the entire landscape of string compactifications. We show that $\gamma\gamma \to e^+e^-$ scattering proceeds only through a spin-2 Regge state. We estimate that for this particular channel, string scales as high as 4 TeV can be discovered at the 11σ level with the first fb^{-1} of data collected at a center-of-mass energy ≈ 5 TeV. We also show that for e^+e^- annihilation into fermion-antifermion pairs, string theory predicts the *precise* value, equal to $1/3$, of the relative weight of spin 2 and spin 1 contributions. This yields a dimuon angular distribution with a pronounced forward-backward asymmetry, which will help distinguishing between low-mass strings and other beyond the standard model scenarios.

DOI: 10.1103/PhysRevD.83.106006 PACS numbers: 11.25.Mj

I. INTRODUCTION

e^+e^- linear colliders are considered to be the most desirable facility to complement measurements at the Large Hadron Collider (LHC). Two alternative linear projects are currently under consideration: the International Linear Collider (ILC) and the Compact LInear Collider (CLIC). The first one is based on superconducting technology in the TeV range, whereas the second one is based on the novel approach of two beam acceleration to extend linear colliders into the multi-TeV range. The choice will be based on the respective maturity of each technology and on the physics requests derived from the LHC physics results when available.

CLIC aims at multi-TeV collision energy with high-luminosity, $\mathcal{L}_{e^+e^-} \sim 8 \times 10^{34}$ cm^{-2} s^{-1} [1]. The facility would be built in phases. The initial center-of-mass energy has been arbitrarily chosen to be $\sqrt{s} = 500$ GeV to allow direct comparison with ILC. The collider design has been optimized for $\sqrt{s} = 3$ TeV, with a possible upgrade path to $\sqrt{s} = 5$ TeV at constant luminosity [2]. To keep the length (and thereby the cost) of the machine at a reasonable level, the CLIC study foresees a two beam accelerating scheme featuring an accelerating gradient in the presence of a beam (loaded) in the order of 80 MV/m and 100 MV/m, for the 500 GeV and 3 TeV options; the projected total site lengths are 13.0 km and 48.3 km, respectively [3]. The CLIC technology is less mature than that of the ILC. In particular, the target accelerating gradient is considerable higher than the ILC and requires very aggressive performance from accelerating structures.

In addition, photon collisions that will considerably enrich the CLIC physics program can be obtained for a relatively small incremental cost. Recently, an exploratory study has been carried out to determine how this facility could be turned into a collider with a high geometric luminosity, which could be used as the basis for a $\gamma\gamma$ collider [4]. The hard photon beam of the $\gamma\gamma$ collider can be obtained by using the laser backscattering technique, i.e., the Compton scattering of laser light on the high energy electrons [5]. The scattered photons have energies close to the energy of the initial electron beams, and the expected $\gamma\gamma$ and γe luminosities can be comparable to that in e^+e^- collisions, e.g., $\mathcal{L}_{\gamma\gamma} \sim 2 \times 10^{34}$ cm^{-2} s^{-1}.

If either supersymmetry (SUSY) or extra dimensions exist at the TeV scale, signals of new physics should be found at the LHC. However, the proper interpretation of such discoveries, namely, the correct identification and the nature of the new physics signals, may not be straightforward at the LHC and may require complementary data from CLIC. In particular, a multi-TeV collider would ensure a sensitivity over a broad mass range allowing a complete investigation of the SUSY particle spectrum [6]. Alternatively, distinct signals of new vector resonances and quantum black holes could also be at reach [7]. Along these lines, in this work we discuss direct searches of string physics at CLIC drawing upon LHC techniques developed elsewhere [8–16].

In string theory, elementary particles are quantized vibrations of fundamental strings. The zero modes are massless, the first harmonics have masses equal to the fundamental mass M, the second $\sqrt{2}M$ and, in general,

$$M_n = \sqrt{n}M. \tag{1}$$

These massive *Regge* particles have higher spins, ranging from 0 to $n+1$ and come in $SU(3) \times SU(1) \times U(1)_Y$ representations copied from gauge bosons, quarks, and leptons. For example, a gluon's lowest Regge excitations are spin 0, 1, and 2 color octets. The standard model (SM) spectrum is replicated at mass M and then at each $\sqrt{n}M$ level. It is possible that loop corrections can split some levels, however this infinite replication is the most fundamental property of string theory.

If, as commonly believed, M is in the Planckian regime, then the landscape problem makes it very difficult to connect string theory to experimental data. However, theoretically M can be as low as few TeVs, provided that nature endowed us with some large extra dimensions, with typical length scale of order 0.1 mm [17]. Such a ''low string mass'' scenario leads to some spectacular experimental consequences, universal to all compactifications, and thus, insensitive to the landscape problem. After operating for only few months, with merely 2.9 inverse picobarns of integrated luminosity, the LHC CMS experiment has recently ruled out $M < 2.5$ TeV by searching for narrow resonances in the dijet mass spectrum [18]. In fact, LHC has the capacity of discovering strongly interacting resonances in practically all range up to $\sqrt{s}_{\rm LHC}$. The present study is based on the optimistic assumption that by the time the ILC/CLIC start operating, there will be at least some indications for the existence of Regge resonances. We will argue that the proposed e^+e^- and $\gamma\gamma$ colliders offer an excellent opportunity for probing string physics.

The layout of the paper is as follows. In Sec. II we outline the basic setting of TeV-scale string compactifications and discuss general aspects of intersecting D-brane configurations that realize the SM by open strings. In Sec. III we present a complete calculation of all relevant four-point string scattering amplitudes. The computation is performed in a model-independent and universal way, and so our results hold for all compactifications. In Sec. IV we discuss the associated phenomenological aspects of Regge recurrences of open strings related to experimental searches for new physics at CLIC. Our conclusions are collected in Sec. V.

II. PHOTON IN THE INTERSECTING BRANE SM CONSTRUCTIONS

TeV-scale superstring theory provides a brane-world description of the SM, which is localized on D-branes extending in $p+3$ spatial dimensions. Gauge interactions emerge as excitations of open strings with endpoints attached on the D-branes, whereas gravitational interactions are described by closed strings that can propagate in all nine spatial dimensions of string theory [these comprise parallel dimensions extended along the $(p+3)$-branes and transverse dimensions].

The basic unit of gauge invariance for D-brane constructions is a $U(1)$ field, and so one can stack up N identical D-branes to generate a $U(N)$ theory with the associated $U(N)$ gauge group. Gauge bosons are due to strings attached to stacks of D-branes and chiral matter due to strings stretching between intersecting D-branes [19]. Each of the two strings' endpoints carries a fundamental charge with respect to the stack of branes on which it terminates. Matter fields carry quantum numbers associated with bifundamental representations.

While the existence of Regge excitations is a completely universal feature of string theory, there are many ways of realizing SM in such a framework. Individual models utilize various D-brane configurations and compactification spaces. They may lead to very different SM extensions, but as far as the collider signatures of Regge excitations are concerned, their differences boil down to a few parameters. The most relevant characteristics are how the $U(1)_Y$ hypercharge is embedded in the $U(1)$'s associated to D-branes. One $U(1)$ (baryon number) comes from the ''QCD'' stack of three branes, as a subgroup of the $U(3)$ group that contains $SU(3)$ color but obviously one needs at least one extra $U(1)$. In D-brane compactifications, hypercharge always appears as a linear, nonanomalous combination of the baryon number with one, two, or more $U(1)$'s. The precise form of this combination bears down on the photon couplings, however, the differences between individual models amount to numerical values of a few parameters. In order to develop our program in the simplest way, we work within the construct of a minimal model in which the color stack a of three D-branes is intersected by the (weak doublet) stack b and by one (weak singlet) D-brane c [20]. For the two-brane stack b, there is a freedom of choosing physical state projections leading either to $U(2)_b$ or to the symplectic $Sp(1)$ representation of Weinberg-Salam $SU(2)_L$ [21].

In the bosonic sector, the open strings terminating on QCD stack a contain the standard $SU(3)$ octet of gluons g_μ^a and an additional $U(1)_a$ gauge boson C_μ, most simply the manifestation of a gauged baryon number symmetry: $U(3)_a \sim SU(3) \times U(1)_a$. On the $U(2)_b$ stack the open strings correspond to the electroweak gauge bosons A_μ^a, and again an additional $U(1)_b$ gauge field X_μ. So the associated gauge groups for these stacks are $SU(3) \times U(1)_a$, $SU(2)_L \times U(1)_b$, and $U(1)_c$, respectively. We can further simplify the model by eliminating X_μ; to this end instead we can choose the projections leading to $Sp(1)$ instead of $U(2)_b$ [21]. The $U(1)_Y$ boson Y_μ, which gauges the usual electroweak hypercharge symmetry, is a linear combination of C_μ, the $U(1)_c$ boson B_μ, and perhaps a third additional $U(1)$ gauge field, X_μ. The fermionic matter consists of open strings located at the intersection points of the three stacks. Concretely, the left-handed quarks are sitting at the intersection of the a and the b stacks, whereas the right-handed u quarks come from the intersection of the a

and c stacks and the right-handed d quarks are situated at the intersection of the a stack with the c' (orientifold mirror) stack. All the scattering amplitudes between these SM particles, which we will need in the following, essentially only depend on the local intersection properties of these D-brane stacks [22].

The chiral fermion spectrum of the $U(3)_a \times Sp(1) \times U(1)_c$ D-brane model is given in Table I. In such a minimal D-brane construction, if the coupling strength of C_μ is down by root six when compared to the $SU(3)_C$ coupling g_a, the hypercharge $Q_Y \equiv \frac{1}{6}Q_{U(3)} - \frac{1}{2}Q_{U(1)}$ is free of anomalies. However, the $Q_{U(3)}$ (gauged baryon number) is anomalous. This anomaly is canceled by the f-D version [23] of the Green-Schwarz mechanism [24]. The vector boson Y'_μ, orthogonal to the hypercharge, must grow a mass in order to avoid long range forces between baryons other than gravity and Coulomb forces. The anomalous mass growth allows the survival of global baryon number conservation, preventing fast proton decay [25].

In the $U(3)_a \times Sp(1)_L \times U(1)_c$ D-brane model, the $U(1)_a$ assignments are fixed (they give the baryon number) and the hypercharge assignments are fixed by SM. Therefore, the mixing angle θ_P between the hypercharge and the $U(1)_a$ is obtained in a similar manner to the way the Weinberg angle is fixed by the $SU(2)_L$ and the $U(1)_Y$ couplings (g_b and g_Y, respectively) in the SM. The Lagrangian containing the $U(1)_a$ and $U(1)_c$ gauge fields is given by

$$\mathcal{L} = g_c \hat{B}_\mu J_B^\mu + \frac{g_a}{\sqrt{6}} \hat{C}_\mu J_C^\mu, \tag{2}$$

where $\hat{B}_\mu = \cos\theta_P Y_\mu + \sin\theta_P Y'_\mu$ and $\hat{C}_\mu = -\sin\theta_P Y_\mu + \cos\theta_P Y'_\mu$ are canonically normalized, and g_c is the coupling strength of the $U(1)_c$ gauge field. Substitution of these expressions into (2) leads to

$$\mathcal{L} = Y_\mu \left(g_c \cos\theta_P J_B^\mu - \frac{g_a}{\sqrt{6}} \sin\theta_P J_C^\mu \right) + Y'_\mu \left(g_c \sin\theta_P J_B^\mu + \frac{g_a}{\sqrt{6}} \cos\theta_P J_C^\mu \right), \tag{3}$$

with $g_c \cos\theta_P J_B^\mu - \frac{1}{\sqrt{6}} g_a \sin\theta_P J_C^\mu = g_Y J_Y^\mu$. We have seen that the hypercharge is anomaly free if $J_Y = \frac{1}{6}J_C^\mu - \frac{1}{2}J_B^\mu$, yielding

TABLE I. The chiral fermion spectrum of the $U(3)_a \times Sp(1)_L \times U(1)_c$ D-brane model is shown.

Name	Representation	$Q_{U(3)}$	$Q_{U(1)}$	Q_Y
U_i	$(\bar{3}, 1)$	-1	1	$-\frac{2}{3}$
D_i	$(\bar{3}, 1)$	-1	-1	$\frac{1}{3}$
L_i	$(1, 2)$	0	1	$-\frac{1}{2}$
E_i	$(1, 1)$	0	-2	1
Q_i	$(3, 2)$	1	0	$\frac{1}{6}$

$$g_c \cos\theta_P = \frac{1}{2} g_Y \quad \text{and} \quad \frac{g_a}{\sqrt{6}} \sin\theta_P = \frac{1}{6} g_Y. \tag{4}$$

From (4) we obtain the following relations:

$$\tan\theta_P = \sqrt{\frac{2}{3}} \frac{g_c}{g_a}, \qquad \left(\frac{g_Y}{2g_c}\right)^2 + \left(\frac{1}{\sqrt{6}} \frac{g_Y}{g_a}\right)^2 = 1, \quad \text{and} \quad \frac{1}{4g_c^2} + \frac{1}{6g_a^2} = \frac{1}{g_Y^2}. \tag{5}$$

We use the evolution of gauge couplings from the weak scale M_Z as determined by the one-loop beta functions of the SM with three families of quarks and leptons and one Higgs doublet,

$$\frac{1}{\alpha_i(M)} = \frac{1}{\alpha_i(M_Z)} - \frac{b_i}{2\pi} \ln\frac{M}{M_Z}; \qquad i = a, b, Y, \tag{6}$$

where $\alpha_i = g_i^2/4\pi$ and $b_a = -7$, $b_b = -19/6$, $b_Y = 41/6$. We also use the measured values of the couplings at the Z pole $\alpha_a(M_Z) = 0.118 \pm 0.003$, $\alpha_b(M_Z) = 0.0338$, $\alpha_Y(M_Z) = 0.01014$ (with the errors in $\alpha_{b,Y}$ less than 1%) [26]. Running couplings up to 3 TeV, which is where the phenomenology will be, we get $\kappa \equiv \sin\theta_P \sim 0.14$. When the theory undergoes electroweak symmetry breaking, because Y' couples to the Higgs, one gets additional mixing. Hence Y' is not exactly a mass eigenstate. The explicit form of the low energy eigenstates A_μ, Z_μ, and Z'_μ is given in [27].

In the $U(3)_a \times U(2)_b \times U(1)_c$ D-brane model, the hypercharge is given by

$$Q_Y = c_a Q_{U(3)} + c_b Q_{U(2)} + c_c Q_{U(1)}. \tag{7}$$

Note that we have, in the covariant derivative $\mathcal{D}_\mu$,

$$\mathcal{D}_\mu = \partial_\mu - i g_c B_\mu Q_{U(1)} - i \frac{g_b}{2} X_\mu Q_{U(2)} - i \frac{g_a}{\sqrt{6}} C_\mu Q_{U(3)}. \tag{8}$$

We can define Y_μ and two other fields Y'_μ, Y''_μ that are related to C_μ, X_μ, B_μ by a orthogonal transformation O defined as

$$\begin{pmatrix} Y \\ Y' \\ Y'' \end{pmatrix} = O \begin{pmatrix} C \\ X \\ B \end{pmatrix}.$$

In order for Y_μ to have the hypercharge Q_Y as in Eq. (7), we need,

$$C_\mu = \frac{\sqrt{6} c_a g_Y}{g_a} Y_\mu + \ldots, \quad X_\mu = \frac{2 c_b g_Y}{g_b} Y_\mu + \ldots, \quad B_\mu = \frac{c_c g_Y}{g_c} Y_\mu + \ldots, \tag{9}$$

where g_Y is given by

$$\frac{1}{g_Y^2} = \frac{6c_a^2}{g_a^2} + \frac{4c_b^2}{g_b^2} + \frac{c_c^2}{g_c^2}. \tag{10}$$

The field Y_μ then appears in the covariant derivative with the desired Q_Y,

$$\mathcal{D}_\mu = \partial_\mu - ig_Y Y_\mu Q_Y + \ldots. \tag{11}$$

The ratio of the coefficients in Eq. (9) is determined by the form of Eqs. (7) and (8). More explicitly, only with such ratio, we can have Q_Y in Eq. (11). The value of g_Y is determined so that the coefficients in Eq. (9) are components of a normalized vector so that they can be a row vector of O. The rest of the transformation (the ellipsis part) involving Y', Y'' is not necessary for our calculation. The point is that we now know the first row of the matrix O and hence we can get the first column of O^T, which gives the expression of Y_μ in terms of C_μ, X_μ, B_μ,

$$Y_\mu = \frac{\sqrt{6}c_a g_Y}{g_a} C_\mu + \frac{2c_b g_Y}{g_b} X_\mu + \frac{c_c g_Y}{g_c} B_\mu. \tag{12}$$

This is all we need when we calculate the interaction involving Y_μ; the rest of O, which tells us the expression of Y', Y'' in terms of C, X, B is not necessary. For later convenience, we define κ, η, ξ as

$$Y_\mu = \kappa C_\mu + \eta X_\mu + \xi B_\mu; \tag{13}$$

therefore

$$\kappa = \frac{\sqrt{6}c_a g_Y}{g_a}, \qquad \eta = \frac{2c_b g_Y}{g_b}, \qquad \xi = \frac{c_c g_Y}{g_c}. \tag{14}$$

We pause to summarize the degree of model dependency stemming from the multiple $U(1)$ content of the minimal model containing 3 stacks of D-branes. First, there is an initial choice to be made for the gauge group living on the b stack. This can be either $Sp(1)$ or $U(2)$. In the case of $Sp(1)$, the requirement that the hypercharge remain anomaly free was sufficient to fix its $U(1)_a$ and $U(1)_c$ content, as explicitly presented in Eqs. (4) and (5). Consequently, the fermion couplings, as well as the mixing angle θ_P between hypercharge and the baryon number gauge field are wholly determined by the usual SM couplings. The alternative selection—that of $U(2)$ as the gauge group tied to the b stack—branches into some further choices. This is because the Q_a, Q_b, Q_c content of the hypercharge operator is not uniquely determined by the anomaly cancellation requirement. In fact, as seen in [20], there are 5 possibilities. This final choice does not depend on further symmetry considerations; in Ref. [20] it was fixed ($c_a = 2/3$, $c_b = 1/2$, $c_c = 1$) by requiring partial unification ($g_a = g_b$) and acceptable value of $\sin^2\theta_W$ at string scales of 6 to 8 TeV. In Ref. [28], a different choice is made ($c_a = -2/3$, $c_b = 1$, $c_c = 0$) to explain the CDF anomaly [29]. Clearly the mixing possibilities within the $U(1)_a \times U(1)_b \times U(1)_c$ serve to introduce a discrete number of phenomenological ambiguities. This contrasts strongly with the case where all the scattering evolves on one brane (e.g., the a stack on the color brane, which serves as the locale for stringy dijet processes at LHC [12]).

In principle, in addition to the orthogonal field mixing induced by identifying anomalous and nonanomalous $U(1)$ sectors, there may be kinetic mixing between these sectors. In our case, however, since there is only one $U(1)$ per stack of D-branes, the relevant kinetic mixing is between $U(1)$'s on different stacks, and hence involves loops with fermions at the brane intersection. Such loop terms are typically down by $g_i^2/16\pi^2 \sim 0.01$ [30]. Generally, the major effect of the kinetic mixing is in communicating SUSY breaking from a hidden $U(1)$ sector to the visible sector, generally in modification of soft scalar masses. Stability of the weak scale in various models of SUSY breaking requires the mixing to be orders of magnitude below these values [30]. For a comprehensive review of experimental limits on the mixing, see [31]. Moreover, the model discussed in the present work does not have a hidden sector—all our $U(1)$'s (including the anomalous ones) couple to the visible sector.[1] In summary, kinetic mixing between the nonanomalous and the anomalous $U(1)$'s in our basic three stack model will be small because the fermions in the loop are all in the visible sector. In the absence of electroweak symmetry breaking, the mixing vanishes.

The scattering amplitudes involving four gauge bosons as well as those with two gauge bosons plus two leptons do not depend on the compactification details of the transverse space [11].[2] They will be particularly useful for testing low-mass strings in $\gamma\gamma$ collisions. On the other hand, the amplitudes involving four fermions, including $e^+e^- \to e^+e^-$, $e^+e^- \to \mu^+\mu^-$, and $e^+e^- \to q\bar{q}$ (in general, $e^+e^- \to F\bar{F}$, where $F\bar{F}$ is a fermion-antifermion pair), which are of particular interest for the e^+e^- collider, depend on the properties of extra dimensions and may include resonant contributions due to Kaluza-Klein excitations, string excitations of the Higgs scalar, etc. However, it follows from Ref. [16] that the three-point couplings of Regge excitations to fermion-antifermion pairs are model-independent. Furthermore, the relative weights of resonances with different spins $J = 0, 1, 2$ are unambiguously predicted by the theory. Thus, the resonant contributions to these amplitudes, with Regge excitations propagating in the s channel, are model independent. e^+e^- colliders can be used not only for discovering such resonances, but most

[1]We also work in the weak coupling regime. For an alternate approach, see [32].

[2]The only remnant of the compactification is the relation between the Yang-Mills coupling and the string coupling. We take this relation to reduce to field theoretical results in the case where they exist, e.g., $gg \to gg$. Then, because of the required correspondence with field theory, the phenomenological results are independent of the compactification of the transverse space. However, a different phenomenology would result as a consequence of warping one or more parallel dimensions [33].

importantly, for detailed studies of their spin content, therefore for distinguishing low-mass string theory from other beyond the SM extensions predicting the existence of similar particles.

III. REGGE RESONANCES IN $\gamma\gamma$ AND e^+e^- CHANNELS

A. Universal amplitudes for $\gamma\gamma$ fusion

1. $\gamma\gamma \to \gamma\gamma$, $\gamma\gamma \to Z^0Z^0$, $\gamma\gamma \to W^+W^-$, $\gamma\gamma \to gg$

As explained in the previous section, the electroweak hypercharge is a linear combination of charges associated to different stacks of D-branes, therefore, photons are linear combinations of three or more vector bosons. On the other hand, at the string disk level, nonvanishing amplitudes with no external particles other than gauge bosons always involve a single stack of D-branes at the disk boundary. Nevertheless, $\gamma\gamma$ fusion into gluon pairs, etc. is possible already at this level because the two initial photons are superpositions of states associated to different stacks. We will first study the resonant behavior of single-stack amplitudes and then compute the weights of the corresponding contributions to $\gamma\gamma$ processes under consideration.

All string disk amplitudes with four external gauge bosons A can be obtained from the MHV amplitude [34][3]:

$$\begin{aligned}\mathcal{M}(A_1^-,A_2^-,A_3^+,A_4^+) &= 4g^2\langle 12\rangle^4\Bigg[\frac{V_t}{\langle 12\rangle\langle 23\rangle\langle 34\rangle\langle 41\rangle}\mathrm{Tr}(T^{a_1}T^{a_2}T^{a_3}T^{a_4}+T^{a_2}T^{a_1}T^{a_4}T^{a_3})+\frac{V_u}{\langle 13\rangle\langle 34\rangle\langle 42\rangle\langle 21\rangle}\mathrm{Tr}(T^{a_2}T^{a_1}T^{a_3}T^{a_4}+T^{a_1}T^{a_2}T^{a_4}T^{a_3})\\ &+\frac{V_s}{\langle 14\rangle\langle 42\rangle\langle 23\rangle\langle 31\rangle}\mathrm{Tr}(T^{a_1}T^{a_3}T^{a_2}T^{a_4}+T^{a_3}T^{a_1}T^{a_4}T^{a_2})\Bigg],\end{aligned} \tag{15}$$

where the string "form factor" functions of the Mandelstam variables s, t, u $(s+t+u=0)$[4] are defined as

$$V_t = V(s,t,u), \qquad V_u = V(t,u,s), \qquad V_s = V(u,s,t), \tag{16}$$

with

$$\begin{aligned}V(s,t,u) &= \frac{su}{tM^2}B(-s/M^2,-u/M^2)\\ &= \frac{\Gamma(1-s/M^2)\Gamma(1-u/M^2)}{\Gamma(1+t/M^2)}.\end{aligned} \tag{17}$$

The amplitudes have s-channel poles at each $s = nM^2$, as seen from the expansion [36]:

$$\begin{aligned}B(-s/M,-u/M^2) = -\sum_{n=0}^{\infty}\frac{M^{2-2n}}{n!}\frac{1}{s-nM^2}\\ \times\Bigg[\prod_{J=1}^{n}(u+M^2J)\Bigg],\end{aligned} \tag{18}$$

reflecting the propagation of resonances with spins up to $n+1$.

We first focus on the lowest $n=1$ resonances. Near $s=M^2$, V_s is regular while

$$V_t \to \frac{u}{s-M^2}, \qquad V_u \to \frac{t}{s-M^2}. \tag{19}$$

Thus, the s-channel pole term of the amplitude (15), relevant to $(--)$ decays of intermediate states, is

$$\mathcal{M}(A_1^-,A_2^-,A_3^+,A_4^+) \to 2g^2\mathcal{C}^{1234}\frac{\langle 12\rangle^4}{\langle 12\rangle\langle 23\rangle\langle 34\rangle\langle 41\rangle}\frac{u}{s-M^2}, \tag{20}$$

where

$$\mathcal{C}^{1234} = 2\,\mathrm{Tr}(\{T^{a_1},T^{a_2}\}\{T^{a_3},T^{a_4}\}) = 16\sum_{a=0}^{N^2-1}d^{a_1a_2a}d^{a_3a_4a}. \tag{21}$$

The amplitude with the s-channel pole relevant to $(+-)$ decays is

$$\mathcal{M}(A_1^-,A_2^+,A_3^+,A_4^-) \to 2g^2\mathcal{C}^{1234}\frac{\langle 14\rangle^4}{\langle 12\rangle\langle 23\rangle\langle 34\rangle\langle 41\rangle}\frac{u}{s-M^2}. \tag{22}$$

In Table II, we list the group factors and couplings [replacing g^2 in Eqs. (20) and (22)] for the single-stack processes contributing to $\gamma\gamma$ fusion into gauge bosons, evaluated according to Eq. (21).[5]

We now proceed to higher level resonances, starting from $n=2$. Three-particle amplitudes involving one level n Regge excitation (gauge index a) and two massless $U(N)$ gauge bosons (gauge indices a_1 and a_2) are even under the world-sheet parity (reversing the order of Chan-Paton factors) for odd n, and odd for even n [16]. As a result, the respective group factors are the symmetric traces $d^{a_1a_2a}$ for odd n and nonabelian structure constants $f^{a_1a_2a}$ for even n,

[3]We use the standard notation of [35], although the gauge group generators are normalized here in a different way, according to $\mathrm{Tr}(T^aT^b) = \frac{1}{2}\delta^{ab}$.

[4]Here, s, t, u refer to parton subprocesses.

[5]As can be seen in Eq. (8) the X_μ and C_μ normalization carries a factor $1/\sqrt{2N}$, which is absent in the B_μ field. Hence, we should recover the $\sqrt{2N}$ factor [to be $B_\mu(\sqrt{2}g_c)/\sqrt{2}Q_{U(1)}$] and use $\sqrt{2}g_c$ in any calculation that follows from a general N.

TABLE II. Group factors and couplings for the pole terms (20) and (22) are shown.

Process	Coupling	$\mathcal{C}^{1234}$
$CC \to gg$	g_a^2	$\frac{2}{3}\delta_{a_3a_4}$
$CC \to CC$	g_a^2	$\frac{2}{3}$
$XX \to XX$	g_b^2	1
$A^3A^3 \to XX$	g_b^2	1
$A^3A^3 \to A^3A^3$	g_b^2	1
$A^3X \to A^3X$	g_b^2	1
$BB \to BB$	$2g_c^2$	2

respectively. For all configurations of initial particles in the processes listed in Table II, $f^{a_1a_2a} = 0$, therefore the corresponding amplitudes have no s-channel poles associated to Regge resonances with even n.[6] For $USp(N)$ groups, the parity assignment is reversed, however, the relevant symmetric trace $d^{33a} = 0$ for $Sp(1)$, therefore, the same conclusion holds for all SM embeddings under consideration.

Thus, in order to observe higher level resonances, $\gamma\gamma$ collisions would have to reach $\sqrt{s} > \sqrt{3}M$, which, due to the recently established $M > 2.5$ TeV bound, translates into $\sqrt{s} > 4.3$ TeV. It is unlikely that such high energies will be reached in the next generation of $\gamma\gamma$ colliders, therefore, from now on our discussion will be limited to the lowest level resonances.

The $\gamma\gamma$ amplitudes are linear combinations of the amplitudes for processes listen in Table II, with the weights determined by the constants κ, η, ξ, cf. Eq. (14), and the Weinberg angle θ_W with

$$C_W = \cos\theta_W, \qquad S_W = \sin\theta_W. \tag{23}$$

For the $U(3)_a \times U(2)_b \times U(1)_c$ minimal model, they are given by

$$\mathcal{M}(\gamma\gamma \to gg) = \kappa^2 {C_W}^2 \mathcal{M}(CC \to gg), \tag{24}$$

$$\begin{aligned}\mathcal{M}(\gamma\gamma \to \gamma\gamma) &= \kappa^4 {C_W}^4 \mathcal{M}(CC \to CC) + 4\eta^2 {S_W}^2 {C_W}^2 \mathcal{M}(XA^3 \to XA^3) + \eta^4 {C_W}^4 \mathcal{M}(XX \to XX) \\ &\quad + {S_W}^4 \mathcal{M}(A^3A^3 \to A^3A^3) + \eta^2 {S_W}^2 {C_W}^2 \mathcal{M}(A^3A^3 \to XX) + \eta^2 {S_W}^2 {C_W}^2 \mathcal{M}(XX \to A^3A^3) \\ &\quad + \xi^4 {C_W}^4 \mathcal{M}(BB \to BB) \\ &= \kappa^4 {C_W}^4 \mathcal{M}(CC \to CC) + 4\eta^2 {S_W}^2 {C_W}^2 \mathcal{M}(XA^3 \to XA^3) \\ &\quad + ({S_W}^4 + \eta^4 {C_W}^4 + 2\eta^2 {S_W}^2 {C_W}^2) \mathcal{M}(XX \to XX) + \xi^4 {C_W}^4 \mathcal{M}(BB \to BB),\end{aligned} \tag{25}$$

$$\begin{aligned}\mathcal{M}(\gamma\gamma \to Z^0Z^0) &= \kappa^4 {C_W}^2 {S_W}^2 \mathcal{M}(CC \to CC) + 4\eta^2 {S_W}^2 {C_W}^2 \mathcal{M}(XA^3 \to XA^3) \\ &\quad + ({S_W}^2 {C_W}^2 + \eta^4 {C_W}^2 {S_W}^2 + \eta^2 {S_W}^4 + \eta^2 {C_W}^4) \mathcal{M}(XX \to XX) + \xi^4 {S_W}^2 {C_W}^2 \mathcal{M}(BB \to BB),\end{aligned} \tag{26}$$

$$\mathcal{M}(\gamma\gamma \to W^+W^-) = \eta^2 {C_W}^2 \mathcal{M}(XX \to W^+W^-) + {S_W}^2 \mathcal{M}(A^3A^3 \to W^+W^-) = (\eta^2 {C_W}^2 + {S_W}^2) \mathcal{M}(XX \to XX). \tag{27}$$

For the $U(3)_a \times Sp(1)_L \times U(1)_c$ D-brane model, $\eta = 0$, $\xi^2 = 1 - \kappa^2$, and all amplitudes involving X or A^3 vanish. We obtain

$$\mathcal{M}(\gamma\gamma \to gg) = \kappa^2 {C_W}^2 \mathcal{M}(CC \to gg), \tag{28}$$

$$\begin{aligned}\mathcal{M}(\gamma\gamma \to \gamma\gamma) &= \kappa^4 {C_W}^4 \mathcal{M}(CC \to CC) \\ &\quad + (1 - \kappa^2)^2 {C_W}^4 \mathcal{M}(BB \to BB),\end{aligned} \tag{29}$$

$$\begin{aligned}\mathcal{M}(\gamma\gamma \to Z^0Z^0) &= {C_W}^2 {S_W}^2 [\kappa^4 \mathcal{M}(CC \to CC) \\ &\quad + (1 - \kappa^2)^2 \mathcal{M}(BB \to BB)],\end{aligned} \tag{30}$$

$$\mathcal{M}(\gamma\gamma \to W^+W^-) = 0. \tag{31}$$

2. $\gamma\gamma \to F\bar{F}$

Since the vertex operators creating chiral matter fermions contain boundary changing operators connecting two different stacks of intersecting D-branes, say a and b, the disk boundary in the amplitudes involving two fermions and two gauge bosons is always attached to two stacks of D-branes. The gauge bosons can couple either to the same stack or to two different stacks. In the latter case, the amplitude with two gauge bosons in the initial state is proportional to V_s, which has no poles in the s channel [11]. The only amplitudes exhibiting s-channel poles involve the two initial gauge bosons associated the same stack, but carry opposite helicities [11]:

[6] For $n = 2$, this has already been checked by explicit computation in Ref. [37].

$$\mathcal{M}(A_1^-, A_2^+, F_3^-, \bar{F}_4^+) = 2g^2 \frac{\langle 13\rangle^2}{\langle 32\rangle\langle 42\rangle}\left[\frac{t}{s} V_t (T^{a_1}T^{a_2})_{\alpha_3\alpha_4} + \frac{u}{s} V_u (T^{a_2}T^{a_1})_{\alpha_3\alpha_4}\right]. \tag{32}$$

The above equation describes the case of stack a, hence the (fermion) spectator indices associated to stack b have been suppressed. The lowest Regge excitations give rise to the pole term

$$\mathcal{M}(A_1^-, A_2^+, F_3^-, \bar{F}_4^+) \to 2g^2 \mathcal{D}^{1234} \frac{\langle 13\rangle^2}{\langle 32\rangle\langle 42\rangle} \frac{tu}{M^2(s - M^2)}, \tag{33}$$

where the group factor

$$\mathcal{D}^{1234} \equiv \{T^{a_1}, T^{a_2}\}_{\alpha_3,\alpha_4}. \tag{34}$$

The group factors and couplings for the processes relevant to $\gamma\gamma \to F\bar{F}$ are listed in Table III.

As in the case of $\gamma\gamma$ fusion into gauge boson pairs, the higher level resonances contributing to $\gamma\gamma \to F\bar{F}$ come from odd n levels only, so here again we limit our discussion to $n = 1$. In the $U(3)_a \times U(2)_b \times U(1)_c$ case, the relevant amplitudes are

$$\begin{aligned}\mathcal{M}(\gamma\gamma \to q_L\bar{q}_R) &= \eta^2 {C_W}^2 \mathcal{M}(XX \to q_L\bar{q}_R) + {S_W}^2 \mathcal{M}(A^3A^3 \to q_L\bar{q}_R) + \kappa^2 {C_W}^2 \mathcal{M}(CC \to q_L\bar{q}_R) \\ &\quad + 2\eta C_W S_W \mathcal{M}(XA^3 \to q_L\bar{q}_R) \\ &= (\eta^2 {C_W}^2 + {S_W}^2)\mathcal{M}(XX \to q_L\bar{q}_R) + \kappa^2 {C_W}^2 \mathcal{M}(CC \to q_L\bar{q}_R) + 2\eta C_W S_W \mathcal{M}(XA^3 \to q_L\bar{q}_R),\end{aligned} \tag{35}$$

$$\mathcal{M}(\gamma\gamma \to q_R\bar{q}_L) = \xi^2 {C_W}^2 \mathcal{M}(BB \to q_R\bar{q}_L) + \kappa^2 {C_W}^2 \mathcal{M}(CC \to q_R\bar{q}_L), \tag{36}$$

$$\begin{aligned}\mathcal{M}(\gamma\gamma \to e_R^+e_L^-) &= \eta^2 {C_W}^2 \mathcal{M}(XX \to e_R^+e_L^-) + {S_W}^2 \mathcal{M}(A^3A^3 \to e_R^+e_L^-) + \xi^2 {C_W}^2 \mathcal{M}(BB \to e_R^+e_L^-) \\ &\quad + 2\eta C_W S_W \mathcal{M}(XA^3 \to e_R^+e_L^-) \\ &= (\eta^2 {C_W}^2 + {S_W}^2)\mathcal{M}(XX \to e_R^+e_L^-) + \xi^2 {C_W}^2 \mathcal{M}(BB \to e_R^+e_L^-) + 2\eta C_W S_W \mathcal{M}(XA^3 \to e_R^+e_L^-),\end{aligned} \tag{37}$$

$$\mathcal{M}(\gamma\gamma \to e_L^+e_R^-) = \xi^2 {C_W}^2 \mathcal{M}(BB \to e_L^+e_R^-). \tag{38}$$

The amplitudes describing neutrino-antineutrino pair production can be obtained from Eqs. (37) and (38) by the replacement $e_L^- \to \nu_L$, $e_R^+ \to \bar{\nu}_R$. For the $U(3)_a \times Sp(1)_L \times U(1)_c$ D-brane model, we obtain

$$\mathcal{M}(\gamma\gamma \to q_L\bar{q}_R) = \kappa^2 {C_W}^2 \mathcal{M}(CC \to q_L\bar{q}_R), \tag{39}$$

$$\mathcal{M}(\gamma\gamma \to q_R\bar{q}_L) = (1 - \kappa^2){C_W}^2 \mathcal{M}(BB \to q_R\bar{q}_L) + \kappa^2 {C_W}^2 \mathcal{M}(CC \to q_R\bar{q}_L), \tag{40}$$

$$\mathcal{M}(\gamma\gamma \to e^\pm e^\mp) = (1 - \kappa^2){C_W}^2 \mathcal{M}(BB \to e^\pm e^\mp), \tag{41}$$

$$\mathcal{M}(\gamma\gamma \to \nu\bar{\nu}) = (1 - \kappa^2){C_W}^2 \mathcal{M}(BB \to \nu\bar{\nu}). \tag{42}$$

TABLE III. Group factors and couplings for the pole terms (33) are shown.

Process	Coupling	$\mathcal{D}^{1234}$
$CC \to q\bar{q}$	g_a^2	$\frac{1}{3}\delta_{\alpha_3\alpha_4}$
$XX \to q_L\bar{q}_R$	g_b^2	$\frac{1}{2}$
$A^3A^3 \to q_L\bar{q}_R$	g_b^2	$\frac{1}{2}$
$A^3X \to u_L\bar{u}_R$	g_b^2	$\frac{1}{2}$
$A^3X \to d_L\bar{d}_R$	g_b^2	$-\frac{1}{2}$
$BB \to q_R\bar{q}_L$	$2g_c^2$	1
$XX \to e_R^+e_L^-$	g_b^2	$\frac{1}{2}$
$A^3X \to e_R^+e_L^-$	g_b^2	$-\frac{1}{2}$
$A^3A^3 \to e_R^+e_L^-$	g_b^2	$\frac{1}{2}$
$XX \to \bar{\nu}_R\nu_L$	g_b^2	$\frac{1}{2}$
$A^3X \to \bar{\nu}_R\nu_L$	g_b^2	$\frac{1}{2}$
$A^3A^3 \to \bar{\nu}_R\nu_L$	g_b^2	$\frac{1}{2}$
$BB \to e_R^+e_L^-$	$2g_c^2$	1
$BB \to e_L^+e_R^-$	$2g_c^2$	2
$BB \to \bar{\nu}_R\nu_L$	$2g_c^2$	1
$BB \to \bar{\nu}_L\nu_R$	$2g_c^2$	2

B. e^+e^- annihilation into gauge bosons and resonant contributions to $e^+e^- \to F\bar{F}$

1. $e^+e^- \to \gamma\gamma$, $e^+e^- \to Z^0Z^0$, $e^+e^- \to Z^0\gamma$, $e^+e^- \to W^+W^-$

Leptons are decoupled from gluons at the disk level because they originate from strings ending on different D-branes. Thus, e^+e^- pairs can annihilate into photons and electroweak bosons only.[7] The corresponding resonance pole terms are obtained by crossing from Eq. (20):

[7] $e^+e^- \to \gamma\gamma$ in a toy, one-stack, stringy model has been discussed in [38].

$$\mathcal{M}([e^{\pm}]_1^-,[e^{\mp}]_2^+,A_3^-,A_4^+,) \to 2g^2\mathcal{D}^{1234}\frac{\langle 13\rangle^2}{\langle 14\rangle\langle 24\rangle} \times \frac{tu}{M^2(s-M^2)}, \quad (43)$$

with the same group factors as in Table III, but running in the time-reversed channels. In the $U(3)_a \times U(2)_b \times U(1)_c$ case, the physical amplitudes for the processes under consideration are

$$\begin{aligned}\mathcal{M}(e_R^+e_L^- \to \gamma\gamma) &= \eta^2 {C_W}^2\mathcal{M}(e_R^+e_L^- \to XX) + {S_W}^2\mathcal{M}(e_R^+e_L^- \to A^3A^3) + \xi^2{C_W}^2\mathcal{M}(e_R^+e_L^- \to BB) \\ &\quad + 2\eta C_W S_W\mathcal{M}(e_R^+e_L^- \to XA^3) \\ &= (\eta^2{C_W}^2 + {S_W}^2)\mathcal{M}(e_R^+e_L^- \to XX) + \xi^2{C_W}^2\mathcal{M}(e_R^+e_L^- \to BB) + 2\eta C_W S_W\mathcal{M}(e_R^+e_L^- \to XA^3), \quad (44)\end{aligned}$$

$$\mathcal{M}(e_L^+e_R^- \to \gamma\gamma) = \xi^2{C_W}^2\mathcal{M}(e_L^+e_R^- \to BB), \quad (45)$$

$$\mathcal{M}(e_R^+e_L^- \to Z^0Z^0) = (\eta^2{S_W}^2 + {C_W}^2)\mathcal{M}(e_R^+e_L^- \to XX) + \xi^2{S_W}^2\mathcal{M}(e_R^+e_L^- \to BB) + 2\eta C_W S_W\mathcal{M}(e_R^+e_L^- \to XA^3), \quad (46)$$

$$\mathcal{M}(e_L^+e_R^- \to Z^0Z^0) = \xi^2{S_W}^2\mathcal{M}(e_L^+e_R^- \to BB), \quad (47)$$

$$\mathcal{M}(e_R^+e_L^- \to Z^0\gamma) = S_W C_W(\eta^2+1)\mathcal{M}(e_R^+e_L^- \to XX) + \xi^2 S_W C_W\mathcal{M}(e_R^+e_L^- \to BB) + \eta({C_W}^2 + {S_W}^2)\mathcal{M}(e_R^+e_L^- \to XA^3), \quad (48)$$

$$\mathcal{M}(e_L^+e_R^- \to Z^0\gamma) = \xi^2 S_W C_W\mathcal{M}(e_L^+e_R^- \to BB), \quad (49)$$

$$\mathcal{M}(e_R^+e_L^- \to W^+W^-) = \mathcal{M}(e_R^+e_L^- \to A^3A^3), \quad (50)$$

$$\mathcal{M}(e_L^+e_R^- \to W^+W^-) = 0. \quad (51)$$

For the $U(3)_a \times Sp(1)_L \times U(1)_c$ D-brane model, we have

$$\mathcal{M}(e_R^+e_L^- \to \gamma\gamma) = \xi^2{C_W}^2\mathcal{M}(e_R^+e_L^- \to BB), \quad (52)$$

$$\mathcal{M}(e_L^+e_R^- \to \gamma\gamma) = \xi^2{C_W}^2\mathcal{M}(e_L^+e_R^- \to BB), \quad (53)$$

$$\mathcal{M}(e_R^+e_L^- \to Z^0Z^0) = \xi^2{S_W}^2\mathcal{M}(e_R^+e_L^- \to BB), \quad (54)$$

$$\mathcal{M}(e_L^+e_R^- \to Z^0Z^0) = \xi^2{S_W}^2\mathcal{M}(e_L^+e_R^- \to BB), \quad (55)$$

$$\mathcal{M}(e_R^+e_L^- \to Z^0\gamma) = \xi^2 S_W C_W\mathcal{M}(e_R^+e_L^- \to BB), \quad (56)$$

$$\mathcal{M}(e_L^+e_R^- \to Z^0\gamma) = \xi^2 S_W C_W\mathcal{M}(e_L^+e_R^- \to BB), \quad (57)$$

$$\mathcal{M}(e_R^+e_L^- \to W^+W^-) = \mathcal{M}(e_R^+e_L^- \to A^3A^3), \quad (58)$$

$$\mathcal{M}(e_L^+e_R^- \to W^+W^-) = 0. \quad (59)$$

2. Resonant contributions to $e^+e^- \to e^+e^-$, $e^+e^- \to \nu\bar{\nu}$, $e^+e^- \to q\bar{q}$

Four-fermion amplitudes [11] are not universal—they depend on the internal radii and other details of extra dimensions already at the disk level. In particular, they contain resonance poles due to Kaluza-Klein excitations. More serious problems though are due to the presence of resonance poles associated to both massless and massive particles that are either unacceptable from the phenomenological point of view, or are expected to receive large mass corrections due to quantum (anomaly) effects, see Ref. [14] for more details. For example, the same Green-Schwarz mechanism that generates nonzero masses for anomalous gauge bosons does also affect the masses of their Regge excitations. For the above reasons, the phenomenological analysis of e^+e^- annihilation into lepton-antilepton pairs will be quite complicated, as described in more detail in the following, Sec. IV B.

Here, we focus on the lowest Regge excitations of the photon and Z^0, remaining in the spectrum of any realistic model. Since we are considering energies far above the electroweak scale, we can replace γ and Z^0 by the neutral gauge bosons of unbroken $SU(2) \times U(1)_Y$.

At the lowest, $n = 1$ level, each gauge boson comes with several Regge excitations with spins ranging from 0 to 2, but only two particles couple to quark-antiquark and lepton-antilepton pairs: one spin 2 boson and one spin 1 vector particle [10]. All three-particle couplings involving one Regge excitation, one fermion and one antifermion have been determined in Ref. [10] by using the factorization methods. These S-matrix elements are completely

sufficient for reconstructing the resonance part of four-fermion amplitudes [10] by using the Wigner matrix techniques. In the center-of-mass frame, the relevant amplitudes can be written as

$$\mathcal{M}(e_L^- e_R^+ \to F_L \bar{F}_R) \to \frac{M^2}{s-M^2}\frac{e^2}{4}\left(\frac{Y_F}{C_W^2}+\frac{I_{3F}}{S_W^2}\right)\left[d^2_{1,1}(\theta)+\frac{1}{3}d^1_{1,1}(\theta)\right], \tag{60}$$

$$\mathcal{M}(e_L^- e_R^+ \to F_R \bar{F}_L) \to \frac{M^2}{s-M^2}\frac{e^2}{4}\frac{Y_F}{C_W^2}\left[d^2_{1,-1}(\theta)+\frac{1}{3}d^1_{1,-1}(\theta)\right], \tag{61}$$

$$\mathcal{M}(e_R^- e_L^+ \to F_L \bar{F}_R) \to \frac{M^2}{s-M^2}\frac{e^2}{2}\frac{Y_F}{C_W^2}\left[d^2_{1,-1}(\theta)+\frac{1}{3}d^1_{1,-1}(\theta)\right], \tag{62}$$

$$\mathcal{M}(e_R^- e_L^+ \to F_R \bar{F}_L) \to \frac{M^2}{s-M^2}\frac{e^2}{2}\frac{Y_F}{C_W^2}\left[d^2_{1,1}(\theta)+\frac{1}{3}d^1_{1,1}(\theta)\right], \tag{63}$$

where Y_F is the fermion hypercharge, I_{3F} is the fermion weak isospin, and

$$d^2_{1,\pm1}(\theta) = \frac{1\pm\cos\theta}{2}(2\cos\theta\mp 1), \qquad d^1_{1,\pm1}(\theta) = \frac{1\pm\cos\theta}{2}, \tag{64}$$

are the spin 2 and spin 1 Wigner matrix elements [39,40], respectively. A very interesting aspect of the above result is that string theory predicts the precise value, equal to 1/3, of the relative weight of spin 2 and spin 1 contributions.

Here again, we would like to stress that although the full four-fermion scattering amplitudes are model-dependent, their resonance parts are universal because the three-particle couplings involving one Regge excitation and two massless particles do not depend on the compactification space [16].

IV. PHENOMENOLOGY

In this section we study the distinct phenomenology of Regge recurrences arising in the $\gamma\gamma$ and e^+e^- beam settings.

A. $\gamma\gamma$ collisions

As an illustration of the CLIC potential to uncover string signals, we focus attention on dominant $\gamma\gamma \to e^+e^-$ scattering, within the context of the $U(3)_a \times Sp(1)_L \times U(1)_c$ D-brane model. Let us first isolate the contribution to the partonic cross section from the first resonant state, B^*. The s-channel pole term of the average square amplitude can be obtained from formula (41) by taking into account all possible initial polarization configurations. However, for phenomenological purposes, the pole needs to be softened to a Breit-Wigner form by obtaining and utilizing the correct total widths of the resonance. After this is done we obtain

$$|\mathcal{M}(\gamma\gamma\to e^+e^-)|^2 = (1+4)(1-\kappa^2)^2 C_W^4 \frac{4g_c^4}{M^4}\left[\frac{ut(u^2+t^2)}{(s-M^2)^2+(\Gamma^{J=2}_{B^*}M)^2}\right], \tag{65}$$

where the factor of $(1+4)$ in the numerator accounts for the fact that the $U(1)_c$ charge of e_R is twice that of e_L. The decay width of B^* is given by

$$\Gamma^{J=2}_{B^*} = \Gamma^{J=2}_{B^*\to l\bar{l}} + \Gamma^{J=2}_{B^*\to q_R\bar{q}_L} + \Gamma^{J=2}_{B^*\to BB} = \frac{g_c^2}{\pi}M\left[\frac{1}{40}\left(\frac{5}{2}N_e+\frac{1}{2}N_\nu+\frac{1}{2}N_q\right)+\frac{1}{5N}\right] = \frac{13}{20}\frac{g_c^2}{4\pi}M, \tag{66}$$

where $N_e = 3$, $N_\nu = 3$, $N_q = 18$. The first term comprises the contribution from the left-handed $(N_e/2)$ and right-handed $(2N_e)$ electrons, the second term $(N_\nu/2)$ comes from the left-handed neutrinos, and the third term $(N_q/2)$ subsume the right-handed quarks.

The total cross section at an e^+e^- linear collider can be obtained by folding $\hat{\sigma}(\hat{s})$ with the photon distribution function [41]

$$\sigma_{\rm tot}(e^+e^-\Rightarrow\gamma\gamma\to e^+e^-) = \int_{M/\sqrt{s}}^{x_{\rm max}} dz \frac{d\mathcal{L}_{\gamma\gamma}}{dz}\hat{\sigma}(\hat{s}=z^2s), \tag{67}$$

where $\hat{s}$ and s indicate, respectively, the center-of-mass energies of the $\gamma\gamma$ and the parent e^+e^- systems and

$$\frac{d\mathcal{L}_{\gamma\gamma}}{dz} = 2z\int_{z^2/x_{\rm max}}^{x_{\rm max}}\frac{dx}{x}f_{\gamma/e}(x)f_{\gamma/e}(z^2/x) \tag{68}$$

is the distribution function of photon luminosity. The energy spectrum of the backscattered photon in unpolarized incoming $e\gamma$ scattering is given by

$$f_{\gamma/e}(x) = \frac{1}{D(\xi)}\left[1-x+\frac{1}{1-x}-\frac{4x}{\xi(1-x)}+\frac{4x^2}{\xi^2(1-x)^2}\right], \quad (x<x_{\rm max}), \tag{69}$$

where $x = 2\omega/\sqrt{s}$ is the fraction of the energy of the incident electron carried by the backscattered photon and $x_{\rm max} = 2\omega_{\rm max}/\sqrt{s} = \xi/(1+\xi)$. For $x > x_{\rm max}$, $f_{\gamma/e} = 0$. The function $D(\xi)$ is defined as

$$D(\xi) = \left(1-\frac{4}{\xi}-\frac{8}{\xi^2}\right)\ln(1+\xi)+\frac{1}{2}+\frac{8}{\xi}-\frac{1}{2(1+\xi)^2}, \tag{70}$$

where $\xi = 2\omega_0\sqrt{s}/m_e{}^2$, m_e, and ω_0 are, respectively, the electron mass and laser-photon energy, and (of course) the incoming electron energy is $\sqrt{s}/2$. In our evaluation, we choose ω_0 such that it maximizes the backscattered photon energy without spoiling the luminosity through e^+e^- pair creation, yielding $\xi = 2(1+\sqrt{2})$, $x_{\max} \simeq 0.83$, and $D(\xi) \approx 1.84$ [42].

We study the signal-to-noise of Regge excitations in data binned according to the invariant mass $M_{e^+e^-}$ of the e^+e^- pair, after setting cuts on the different electron-positron rapidities, $|y_1|$, $|y_2| \leq 2.4$ and transverse momenta $p_T^{1,2} > 50$ GeV. With the definitions $Y \equiv \frac{1}{2}(y_1 + y_2)$ and $y \equiv \frac{1}{2} \times (y_1 - y_2)$, the cross section per interval of $M_{e^+e^-}$ for $\gamma\gamma \to e^+e^-$ is given by

$$\frac{d\sigma}{dM_{e^+e^-}} = \sqrt{s}z^3\left[\int_{-Y_{\max}}^{0} dY f_{\gamma/e}(x_a) f_{\gamma/e}(x_b) \int_{-(y_{\max}+Y)}^{y_{\max}+Y} dy \frac{d\hat{\sigma}}{d\hat{t}}\bigg|_{\gamma\gamma\to e^+e^-} \frac{1}{\cosh^2 y} + \int_{0}^{Y_{\max}} dY f_{\gamma/e}(x_a) f_{\gamma/e}(x_b) \times \int_{-(y_{\max}-Y)}^{y_{\max}-Y} dy \frac{d\hat{\sigma}}{d\hat{t}}\bigg|_{\gamma\gamma\to e^+e^-} \frac{1}{\cosh^2 y}\right], \tag{71}$$

where $z^2 = M^2_{e^-e^-}/s$, $x_a = ze^Y$, $x_b = ze^{-Y}$, and

$$|\mathcal{M}(\gamma\gamma \to e^+e^-)|^2 = 16\pi\hat{s}^2 \frac{d\sigma}{d\hat{t}}\bigg|_{\gamma\gamma\to e^+e^-}. \tag{72}$$

The string signal is calculated using (71) with the corresponding $\gamma\gamma \to e^+e^-$ scattering amplitude given in Eq. (65). The SM background is calculated using

$$\frac{d\hat{\sigma}}{d\hat{t}} = \frac{2\pi\alpha^2}{\hat{s}^2}\left(\frac{\hat{u}}{\hat{t}} + \frac{\hat{t}}{\hat{u}}\right). \tag{73}$$

The kinematics of the scattering also provides the relation $M_{e^+e^-} = 2p_T \cosh y$, which when combined with the standard cut $p_T \gtrsim p_{T,\min}$, imposes a *lower* bound on y to be implemented in the limits of integration. The Y integration range in Eq. (71), $Y_{\max} = \min\{\ln(x_{\max}/z), y_{\max}\}$, comes from requiring x_a, $x_b < x_{\max}$ together with the rapidity cuts $0 < |y_1|$, $|y_2| < 2.4$. Finally, the Mandelstam invariants occurring in the cross section are given by $\hat{s} = M^2_{e^+e^-}$, $\hat{t} = -\frac{1}{2}M^2_{e^+e^-}e^{-y}/\cosh y$, and $\hat{u} = -\frac{1}{2}M^2_{e^+e^-}e^{+y}/\cosh y$. In Fig. 1 we show a representative plot of the invariant mass spectrum, for $M = 4$ TeV and $\sqrt{s} = 5$ TeV.

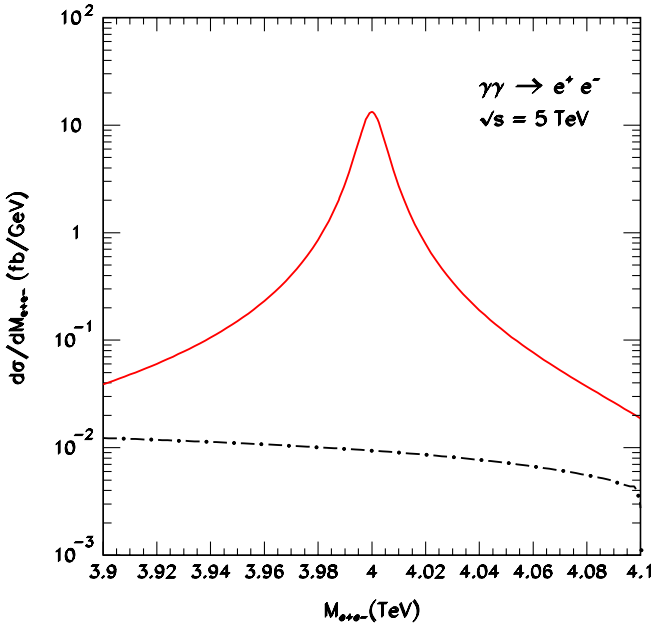

FIG. 1 (color online). $d\sigma/dM_{e^+e^-}$ (units of fb/GeV) vs $M_{e^+e^-}$ (TeV) is plotted for the case of SM background (dot-dashed line) and (first resonance) string signal + background (solid line), for $M = 4$ TeV and $\sqrt{s} = 5$ TeV. (We have taken $\kappa = 0.14$.)

We now estimate (at the parton level) the signal-to-noise ratio at CLIC. Standard bump-hunting methods, such as obtaining cumulative cross sections, $\sigma(M_0) = \int_{M_0}^{\infty} \frac{d\sigma}{dM_{e^+e^-}} dM_{e^+e^-}$, from the data and searching for regions with significant deviations from the SM background, may reveal an interval of $M_{e^+e^-}$ suspected of containing a bump. With the establishment of such a region, one may calculate the detection significance

$$S_{\text{det}} = \frac{N_S}{\sqrt{N_B + N_S}}, \tag{74}$$

with the signal rate N_S estimated in the invariant mass window $[M - 2\Gamma, M + 2\Gamma]$, and the number of background events N_B defined in the same e^+e^- mass interval for the same integrated luminosity [43]. For $\sqrt{s} = 5$ TeV and $M_s = 4$ TeV we expect $S_{\text{det}} \simeq 139/12 = 11\sigma$, after the first fb^{-1} of data collection. The spin-2 nature of $\gamma\gamma \to e^+e^-$ Regge recurrences would make them smoking guns for low-mass scale D-brane string compactifications.

B. e^+e^- collisions

We assume that the e^+e^- center-of-mass energy will be tuned to contain the interesting range highlighted by LHC data and that the resolution of the machine will be sufficient to probe narrow resonances. We are interested in the e^+e^- annihilation into lepton-antilepton pairs, in particular, in $e^-e^+ \to \mu^-\mu^+$. The phenomenological analysis of such processes will be quite complicated, due the presence of model-dependent backgrounds of Kaluza-Klein (KK) excitations, anomalous gauge bosons and their Regge excitations. Weakly interacting KK excitations are expected to have masses lower than the string scale [14], and can appear as resonances in the e^+e^- annihilation channel. Their signals will be similar to a generic Z', with a unique angular momenta, commonly $J = 1$ and will not provide

direct evidence for the superstring substructure. The signals of gauge bosons associated to anomalous $U(1)$ gauge bosons, with masses always lower than the string scale, varying from a loop factor to a large suppression by the volume of the bulk [44], will have a similar character. We assume that no accidental degeneracy occurs between these particles and Regge excitations, so that the string signal discussed Sec. III B 2 can be safely isolated from the background. Even in this case, however, there is a certain amount of ambiguity due to the presence of Regge excitations of anomalous $U(1)$'s with masses shifted by radiative corrections [45]. If this shift is large, there will be a separate resonance peak, but if it is small, it will affect the normalization of the signal.

Should a resonance be found, a strong discriminator between models will be the observed angular distribution. Typical candidates for new physics such as Z' will have a unique angular momenta, commonly $J = 1$. It is an interesting and exciting peculiarity of Regge recurrences that the angular momenta content of the energy state is more complicated. As we have shown in Sec. III B 2, for the lightest Regge excitation there is a specific combination of $J = 1$ and $J = 2$, which are accessed by the e^+e^- beam setting. Specializing at this point to $e^-e^+ \to \mu^-\mu^+$, so that $I_{3F_L} = Y_{F_L} = \frac{1}{2}Y_{F_R} = -1/2$, we obtain the normalized angular distribution

$$\frac{d\sigma/d\cos\theta}{\sigma} = \mathcal{N}\left\{\left[4 + \left(\frac{1}{2S_W^2}\right)^2\right]D_+(\theta)^2 + 2D_-(\theta)^2\right\}, \tag{75}$$

where

$$D_\pm(\theta) \equiv d^2_{1,\pm1}(\theta) + \tfrac{1}{3}d^1_{1,\pm1}(\theta) \tag{76}$$

and

$$\mathcal{N}^{-1} = (64/135)\left[6 + \left(\frac{1}{2S_W^2}\right)^2\right]. \tag{77}$$

For the $J = 2$ piece alone, the normalization constant is

$$\mathcal{N}_2^{-1} = (2/5)\left[6 + \left(\frac{1}{2S_W^2}\right)^2\right], \tag{78}$$

whereas for the $J = 1$ piece alone, the normalization constant is

$$\mathcal{N}_1^{-1} = (2/27)\left[6 + \left(\frac{1}{2S_W^2}\right)^2\right]. \tag{79}$$

In Fig. 2 we show the resulting angular distributions. The predicted dimuon angular distribution has a pronounced forward-backward asymmetry. This is a realistic target for CLIC searches of low-mass scale string theory signals. (Note that the $e^+e^- \to e^+e^-$ Coulomb scattering background, which peaks in the forward direction, tends to wash out the predicted string signal.) In Fig. 3 we show the binned angular distributions. It is clearly seen that it would be easy to distinguish the string excitation from single $J = 2$ resonance in the dimuon angular distribution. To completely isolate the Regge excitation from a $J = 1$ resonance, one can use string predictions in alternative channels, e.g, $\gamma\gamma \to e^+e^-$.

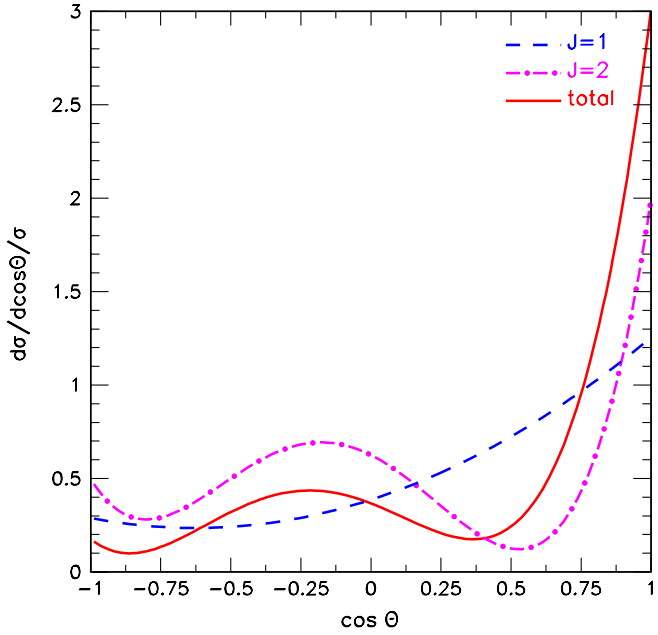

FIG. 2 (color online). Normalized angular distributions of Regge recurrences with spin 1, 2, and total in the $e^+e^- \to \mu^+\mu^-$ channel are shown.

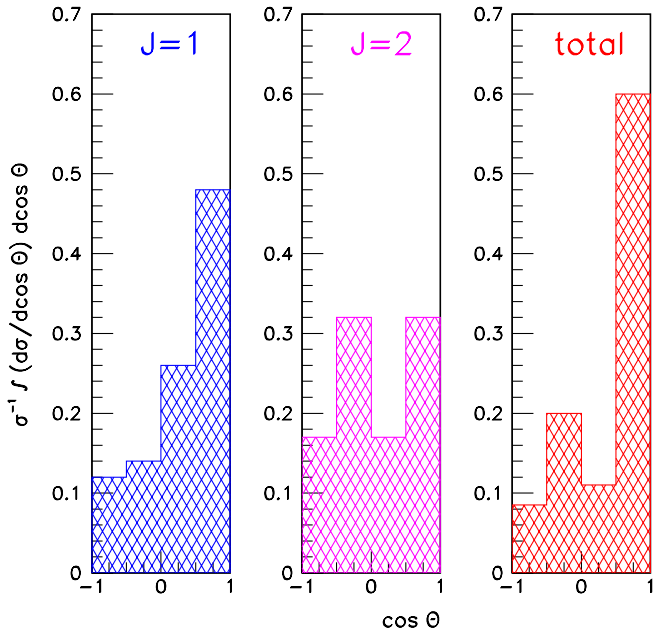

FIG. 3 (color online). Binned angular distributions of Regge recurrences with spin 1, 2, and total in the $e^+e^- \to \mu^+\mu^-$ channel are shown.

V. CONCLUSIONS

In this paper, we have explored the discovery potential of the proposed e^+e^- and $\gamma\gamma$ colliders to unmask string resonances. We have studied the direct production of Regge excitations, focusing on the first excited level of open strings localized on the worldvolume of D-branes. In such a D-brane construction the resonant parts of the relevant string theory amplitudes are universal to leading order in the gauge coupling. Therefore, it is feasible to extract genuine string effects which are independent of the compactification scheme. Among the various processes, we found that the $\gamma\gamma \to e^+e^-$ scattering proceeds only through a spin-2 Regge state. Our detailed phenomenological studies suggest that for this specific channel, string scales as high as 4 TeV can be unmasked at the 11σ level with the first fb^{-1} of data collected at $\sqrt{s} \approx 5$ TeV. We have also investigated intermediate Regge states of $e^+e^- \to F\bar{F}$ and we have shown that string theory predicts the precise value, equal to $1/3$, of the relative weight of spin 2 and spin 1 contributions. The potential benefit of this striking result becomes evident when analyzing the di-muon angular distribution, which has a pronounced forward-backward asymmetry, providing a very distinct signal of the underlying string physics.

ACKNOWLEDGMENTS

We are very grateful to Maria Krawczyk for her encouragement to pursue this project. L. A. A. is supported by the U.S. National Science Foundation (NSF) Grant No. PHY-0757598, and the UWM Research Growth Initiative. W-Z. F., H. G., and T. R. T. are supported by the U.S. NSF Grant No. PHY-0757959. Any opinions, findings, and conclusions or recommendations expressed in this material are those of the authors and do not necessarily reflect the views of the National Science Foundation.

[1] J. R. Ellis and I. Wilson, Nature (London) **409**, 431 (2001); D. Asner *et al.*, Eur. Phys. J. C **28**, 27 (2003).
[2] E. Accomando *et al.* (CLIC Physics Working Group), arXiv:hep-ph/0412251.
[3] J. Ellis, arXiv:0811.1366.
[4] V. I. Telnov, arXiv:0908.3136.
[5] I. F. Ginzburg, G. L. Kotkin, V. G. Serbo, and V. I. Telnov, Pis'ma Zh. Eksp. Teor. Fiz. **34**, 514 (1981) [JETP Lett. **34**, 491 (1981)]; Nucl. Instrum. Methods Phys. Res. **205**, 47 (1983); I. F. Ginzburg, G. L. Kotkin, S. L. Panfil, V. G. Serbo, and V. I. Telnov, Nucl. Instrum. Methods Phys. Res., Sect. A **219**, 5 (1984).
[6] M. Battaglia and M. Gruwe, arXiv:hep-ph/0212140; M. Battaglia, A. Datta, A. De Roeck, K. Kong, and K. T. Matchev, J. High Energy Phys. 07 (2005) 033.
[7] M. Battaglia, A. De Roeck, and T. Rizzo, arXiv:hep-ph/0309022.
[8] L. A. Anchordoqui, H. Goldberg, S. Nawata, and T. R. Taylor, Phys. Rev. Lett. **100**, 171603 (2008).
[9] L. A. Anchordoqui, H. Goldberg, S. Nawata, and T. R. Taylor, Phys. Rev. D **78**, 016005 (2008).
[10] L. A. Anchordoqui, H. Goldberg, and T. R. Taylor, Phys. Lett. B **668**, 373 (2008).
[11] D. Lüst, S. Stieberger, and T. R. Taylor, Nucl. Phys. **B808**, 1 (2009).
[12] L. A. Anchordoqui, H. Goldberg, D. Lüst, S. Nawata, S. Stieberger, and T. R. Taylor, Phys. Rev. Lett. **101**, 241803 (2008).
[13] D. Lust, O. Schlotterer, S. Stieberger, and T. R. Taylor, Nucl. Phys. **B828**, 139 (2010).
[14] L. A. Anchordoqui, H. Goldberg, D. Lust, S. Nawata, S. Stieberger, and T. R. Taylor, Nucl. Phys. **B821**, 181 (2009).
[15] L. A. Anchordoqui, H. Goldberg, D. Lust, S. Stieberger, and T. R. Taylor, Mod. Phys. Lett. A **24**, 2481 (2009).
[16] W. Z. Feng, D. Lust, O. Schlotterer, S. Stieberger, and T. R. Taylor, Nucl. Phys. **B843**, 570 (2011).
[17] I. Antoniadis, N. Arkani-Hamed, S. Dimopoulos, and G. R. Dvali, Phys. Lett. B **436**, 257 (1998).
[18] V. Khachatryan *et al.* (CMS Collaboration), Phys. Rev. Lett. **105**, 211801 (2010); **106**, 029902(E) (2011).
[19] R. Blumenhagen, B. Körs, D. Lüst, and S. Stieberger, Phys. Rep. **445**, 1 (2007).
[20] I. Antoniadis, E. Kiritsis, and T. N. Tomaras, Phys. Lett. B **486**, 186 (2000).
[21] D. Berenstein and S. Pinansky, Phys. Rev. D **75**, 095009 (2007).
[22] For further details on D-brane models see, e.g., F. G. Marchesano Buznego, arXiv:hep-th/0307252.
[23] E. Witten, Phys. Lett. **149B**, 351 (1984); M. Dine, N. Seiberg, and E. Witten, Nucl. Phys. **B289**, 589 (1987); J. J. Atick, L. J. Dixon, and A. Sen, Nucl. Phys. **B292**, 109 (1987); W. Lerche, B. E. W. Nilsson, A. N. Schellekens, and N. P. Warner, Nucl. Phys. **B299**, 91 (1988).
[24] M. B. Green and J. H. Schwarz, Phys. Lett. **149B**, 117 (1984).
[25] D. M. Ghilencea, L. E. Ibanez, N. Irges, and F. Quevedo, J. High Energy Phys. 08 (2002) 016.
[26] C. Amsler *et al.* (Particle Data Group), Phys. Lett. B **667**, 1 (2008).
[27] D. Berenstein, R. Martinez, F. Ochoa, and S. Pinansky, Phys. Rev. D **79**, 095005 (2009).
[28] L. A. Anchordoqui, H. Goldberg, X. Huang, D. Lust, and T. R. Taylor, arXiv:1104.2302.
[29] T. Aaltonen *et al.* (CDF Collaboration), Phys. Rev. Lett. **106**, 171801 (2011)
[30] K. R. Dienes, C. F. Kolda, and J. March-Russell, Nucl. Phys. **B492**, 104 (1997).
[31] S. A. Abel, M. D. Goodsell, J. Jaeckel, V. V. Khoze, and A. Ringwald, J. High Energy Phys. 07 (2008) 124.

[32] N. Kitazawa, Int. J. Mod. Phys. A **25**, 2679 (2010).
[33] B. Hassanain, J. March-Russell, and J. G. Rosa, J. High Energy Phys. 07 (2009) 077; M. Perelstein and A. Spray, J. High Energy Phys. 10 (2009) 096; L. A. Anchordoqui, H. Goldberg, X. Huang, and T. R. Taylor, Phys. Rev. D **82**, 106010 (2010).
[34] S. Stieberger and T. R. Taylor, Phys. Rev. D **74**, 126007 (2006); Phys. Rev. Lett. **97**, 211601 (2006).
[35] M. L. Mangano and S. J. Parke, Phys. Rep. **200**, 301 (1991); L. J. Dixon, arXiv:hep-ph/9601359.
[36] G. Veneziano, Nuovo Cimento A **57**, 190 (1968).
[37] Z. Dong, T. Han, M. x. Huang, and G. Shiu, J. High Energy Phys. 09 (2010) 048.
[38] S. Cullen, M. Perelstein, and M. E. Peskin, Phys. Rev. D **62**, 055012 (2000).
[39] E. P. Wigner, *Group Theory* (Academic Press, New York, 1959).
[40] A. R. Edmonds, *Angular Momentum in Quantum Mechanics* (Princeton University Press, Princeton, 1957).
[41] G. V. Jikia, Nucl. Phys. **B374**, 83 (1992); O. J. P. Eboli, M. C. Gonzalez-Garcia, F. Halzen, and S. F. Novaes, Phys. Rev. D **47**, 1889 (1993).
[42] K. m. Cheung, Phys. Rev. D **47**, 3750 (1993).
[43] L. Anchordoqui, F. Halzen, T. Montaruli, and A. O'Murchadha, Phys. Rev. D **76**, 067301 (2007); **77**, 069906(E) (2008).
[44] I. Antoniadis, E. Kiritsis, and J. Rizos, Nucl. Phys. **B637**, 92 (2002).
[45] N. Kitazawa, J. High Energy Phys. 10 (2010) 051.